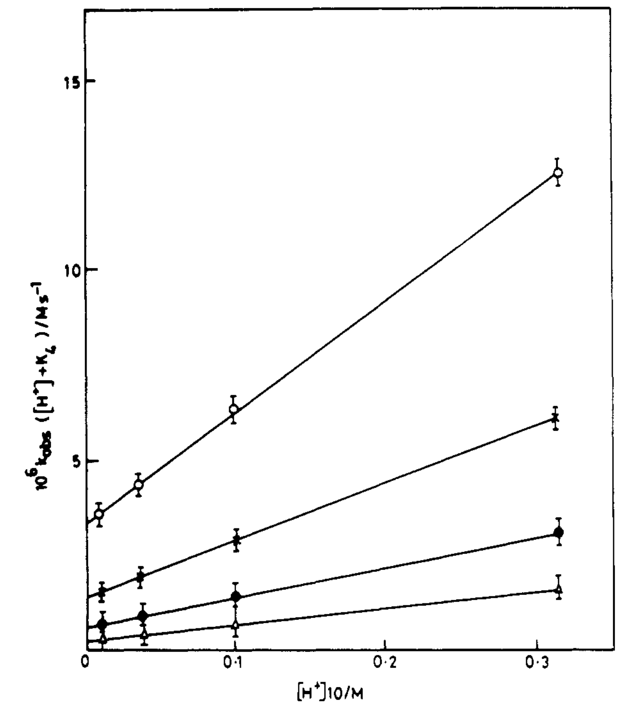

Figure 1. Acid dependence of observed rate constants, k_{obsd}, for the chelation reaction of *cis*-chloro(oxalato)tetraamminechromium(III) at various temperatures. T (°C): (○) 60; (×) 55; (●) 50; (△) 45.

chelation process may be treated as parallel reactions under these conditions as shown in eq 1 and 2.

$$Cr(NH_3)_4(X)(C_2O_4H)^+ \xrightarrow{k_1} Cr(NH_3)_4(C_2O_4)^+ + X^- + H^+ \quad (1)$$

$$Cr(NH_3)_4(X)(C_2O_4H)^+ \xrightarrow{k_2} Cr(NH_3)_3(X)(C_2O_4) + NH_4^+ \quad (2)$$

The rate constant, k_{obsd}, for the first-order decay of $Cr(NH_3)_4(X)(C_2O_4H)^+$ under any condition is therefore given by eq 3 and the product ratio, R, by k_1/k_2. The values of k_1 and

$$k_{obsd} = k_1 + k_2 \quad (3)$$

k_2 may be obtained from k_{obsd} by using the experimental values of R, and the values of k_{obsd}, k_1, and k_2 at 50 °C for various [H$^+$] are also listed in Table II.

It is evident from Tables II and III that, under all conditions, halide substitution during chelation is the more favored process. Although the formation of $Cr(NH_3)_4(C_2O_4)^+$ does involve the displacement of chloride, the intermediacy of any aquo derivative like $Cr(NH_3)_4(H_2O)(C_2O_4H)^{2+}$ (**1**) needs to be ruled out only through other scavenging experiments. This was achieved by using nitrite as a scavenger for any aquo derivative formed during chelation at [H$^+$] = (3–5) × 10^{-4} M. Nitrite is known to undergo substitution with metal–oxygen bond retention and N–O bond breaking.[10] Therefore, if aquo compounds like $Cr(NH_3)_4(H_2O)(C_2O_4H)^{2+}$ or $Cr(NH_3)_4(H_2O)(C_2O_4)^+$ were formed, nitrito oxalato derivatives with charge-transfer bands would be expected. There is no evidence for the formation of such nitrito derivatives, and the rate of release of Cl^- paralleled the values of k_1 obtained in our study. Therefore the values of k_1 and k_2 may be assigned to the rate of direct displacement of a halide by the chelating arm of oxalate. The coordinated oxalate anions are known to exhibit protonation behavior in the [H$^+$] region of our study.[11,12] The values of k_{obsd}, k_1, and k_2 exhibited an [H$^+$] dependence typical of equilibrium 4, influencing rate constants for chelation process.

$$Cr(NH_3)_4(X)(C_2O_4H)^+ \overset{K_4}{\rightleftharpoons} Cr(NH_3)_4(X)(C_2O_4) + H^+ \quad (4)$$

The plots of $k_{obsd}([H^+] + K_4)$ against [H$^+$] were linear and are shown in Figure 1 for the chloride system. Similar results were also observed when $([H^+] + K_4)k_1$ or $([H^+] + K_4)k_2$ was plotted against [H$^+$] when $K_4 = 4.9 \times 10^{-3}$ M at 50 °C and X = Cl or Br. Statistical analysis of k_1 and k_2 using the rate laws of the form shown in eq 5, run on an IBM 370 computer and Los Almos

$$k_1 \text{ or } k_2 = \frac{a[H^+] + bK_4}{[H^+] + K_4} \quad (5)$$

program, gave the values of a and b. The values of a and b correspond to the first-order rate constants for the halide as well as ammonia displacements at 50 °C from dissociated and undissociated oxalato tetraammine derivatives and are listed in Table III. The similarity of rate constants observed in this study for the reaction of protonated and dissociated forms is as reported earlier for other related systems.[11]

It is evident from Table III that direct substitution of halide by the dissociated arm of oxalate does occur in preference to the substitution of neutral ammonia ligand, and the rate constants for the displacement of Cl^- and Br^- by carboxylates in the oxalato derivatives studied in case of oxalato-*O,O'* derivatives are nearly the same. The activation parameters obtained for various pathways show that ammonia displacement has a higher enthalpy of activation ΔH (ca. 2.5–5.0 kcal mol^{-1} higher than that for halide displacement).[12] Therefore entropy advantages that anions may enjoy against their direct substitution by another anion do not seem to override the enthalpic components to substitution reactivity, even when associate pathways occur.

Registry No. *cis*-$Cr(NH_3)_4Cl(C_2O_4H)^+$, 104130-06-5; *cis*-$Cr(NH_3)_4Br(C_2O_4H)^+$, 104130-07-6; Cl_2, 7782-50-5; Br_2, 7726-95-6; NH_3, 7664-41-7.

(10) (a) Basolo, F.; Hammaker, *Inorg. Chem.* **1962**, *1*, 1. (b) Matts, T. C.; Moore, P. *J. Chem. Soc. A* **1971**, 1632. (c) The reactions of aquo complexes like $Cr(H_2O)_6^{3+}$ with nitrite have been shown to be relatively rapid.

(11) (a) Ramasami, T.; Wharton, R. K.; Sykes, A. G. *Inorg. Chem.* **1975**, *14*, 359. (b) Andrade, C.; Taube, H. *Inorg. Chem.* **1966**, *5*, 1087.

(12) Narayanaswamy, C.; Ramasami, T.; Ramaswamy, D., unpublished results.

Contribution from the Science Research Laboratory, 3M Corporate Research Laboratories, St. Paul, Minnesota 55144

Ternary Rhodium–Tungsten–Sulfur Clusters

A. R. Siedle* and W. B. Gleason

Received March 25, 1986

We have previously reported the syntheses and structures of clusters and nets derived from the dithiotungstate(2–), $WO_2S_2^{2-}$, and tetrathiotungstate(2–), WS_4^{2-}, ions and metals of the copper group (Cu, Ag, Au). Exemplary are $[(Ph_2PMe)Au]_2WS_4$,[1] in which gold bridges alternate edges of the WS_4 tetrahedron to form a netlike structure; $([(Ph_2PMe)Ag]_2WS_4)_2$[2] and $([(p\text{-tolyl})_3PCu]_2WOS_3)_2$,[3] which contain 12-atom cages formed by dimerization of units in which two metals bridge adjacent edges on the thiometalate tetrahedra; and $(Et_3P)_2PtWS_4$,[4] in which

(1) Huffman, J. C.; Roth, R. S.; Siedle, A. R. *J. Am. Chem. Soc.* **1976**, *98*, 4340.
(2) Stalick, J. K.; Siedle, A. R.; Mighell, A. D.; Hubbard, C. R. *J. Am. Chem. Soc.* **1979**, *101*, 2832.
(3) Doherty, R.; Hubbard, C. R.; Mighell, A. D.; Siedle, A. R. *Inorg. Chem.* **1979**, *18*, 2991.
(4) Siedle, A. R.; Hubbard, C. R.; Mighell, A. D.; Stewart, J. D.; Doherty, R. *Inorg. Chim. Acta* **1980**, *38*, 197.

0020-1669/86/1325-4054$01.50/0

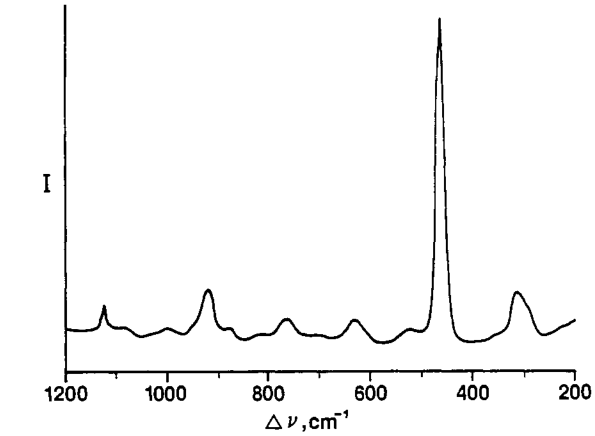

Figure 1. Resonance Raman spectrum of $[(diphos)Rh]_2WS_4$ (**7**).

platinum bridges one tetrahedral edge. We have expanded these studies to include chemical and crystallographic characterization of Rh(I) and Ir(I) derivatives, which are the topic of this paper.[5,6] An additional motivation for this work was obtention of structural data for rhodium–tungsten compounds for use as standards in our EXAFS studies of molecular metal oxide clusters containing $(Ph_3P)_2Rh(CO)$ groups.[7]

Results and Discussion

Reaction of the cationic 14-electron Rh(I) compound $[(Ph_3P)_3Rh]^+[HC(SO_2CF_3)_2]^-$[8,9] with $Ph_3PCH_3^+$ or Ph_4As^+ salts of WS_4^{2-} or MoS_4^{2-} in dichloromethane affords $[(Ph_3P)_2Rh]_2WS_4$ (**1**) ($\delta(^{31}P)$ 42.8 (J_{PRh} = 173 Hz); λ_{max} 534 nm (log ϵ = 4.00)) and $[(Ph_3P)_2Rh]_2MoS_4$ (**2**) ($\delta(^{31}P)$ 44.6 (J_{PRh} = 170 Hz); λ_{max} 430 (3.80) and 670 nm (3.94)), respectively. The dithiomolybdate complex $[(Ph_3P)_2Rh]_2MoO_2S_2$ (**3**) (λ_{max} 570 nm (3.49)), was similarly prepared from $(Ph_3PCH_3)_2MoO_2S_2$. These rhodium tetrathiometalates are obtained as dark purple or violet microcrystalline solids whose electronic spectra exhibit long wavelength absorptions (>500 nm). These bands may be attributed to Rh(I) → W(VI) charge-transfer processes as they shift to higher energy when one or both Ph_3P ligands are replaced by the more strongly π-accepting 1,5-cyclooctadiene or carbon monoxide (vide infra). In an alternate, plausible description, suggested by a reviewer, a $5d_{z^2}$ orbital on tungsten can mix with $4d_{xy}$ orbitals on rhodium to form one bonding, one nonbonding, and one antibonding orbital. With four electrons available from the two Rh d_{xy} orbitals, the bonding and nonbonding MO's would be filled, giving a net W–Rh bond order of 0.5; the 500-nm absorption could then be assigned to a bonding (or nonbonding) to antibonding MO transition. Detailed molecular orbital calculations will likely be required to distinguish between these two possibilities.

Infrared spectra show bands in the ~470-cm^{-1} region due to W–S stretching. The ^{31}P NMR spectra of **1** and **2** are simple doublets, but that of **3** is an ABX pattern (δ_A 31.3, δ_B 43.7, J_{AB} = 36 Hz, J_{AX} = 177 Hz, and J_{BX} = 170 Hz) because the nonequivalent Ph_3P ligands are trans to oxygen or to sulfur. Unfortunately, it is not clear how to unambiguously assign the spectrum.

Reaction of **1** with excess carbon monoxide leads to displacement of only one triphenylphosphine ligand from each rhodium center and yields orange $[Ph_3PRh(CO)]_2WS_4$ (**4**) (ν_{CO} 2008 cm^{-1} (toluene); $\delta(^{13}C)$ 189.5 (J_{CRh} = 73 Hz); $\delta(^{31}P)$ 35.8 (J_{PRh} = 154 Hz); λ_{max} 474 nm (3.81, toluene solution)). Alternatively, **4** may be obtained from $[(Ph_3P)_3Rh(CO)_2]^+[HC(SO_2CF_3)_2]^-$[8,9] and $(Ph_3PCH_3)_2WS_4$. The molybdenum analogue of **4** has lower stability and was not isolated in analytically pure form.

Displacement of chloride from $[(C_8H_{12})MCl]_2$ (M = Rh, Ir) using $(Ph_4As)_2WS_4$ produces orange $[(C_8H_{12})Rh]_2WS_4$ (**5**) (λ_{max} 465 nm (3.90)) and $[(C_8H_{12})Ir]_2WS_4$ (**6**) (λ_{max} 510 nm (3.73)), respectively. The cyclooctadiene ligand in **6** is relatively labile and may be displaced with 1,2-bis(diphenylphosphino)ethane (diphos) to provide carmine $[(diphos)Rh]_2WS_4$ (**7**) ($\delta(^{31}P)$ 70.3 (J_{PRh} = 165 Hz); λ_{max} 510 nm (3.73)). Using Ph_2PCH_3 instead yields purple $[(Ph_2PCH_3)_2Rh]_2WS_4$, which is unstable in air. Unlike $[CpRu(PPh_3)]_2WS_4$, **7** is electrochemically inactive.[5]

The Raman spectra of **1**, **2**, **5**, **6**, and **7** reveal strong bands near 310 and 470 cm^{-1} assigned to Rh–S and W–S stretching, respectively. The ν(Rh–S) band is expected to lie below ν(W–S) on account of the formal oxidation state difference (+1, +6) between the total metal centers.[10,11] The spectra also exhibit

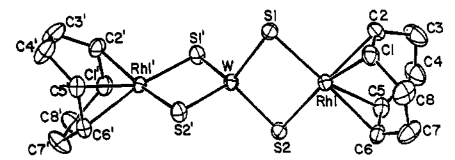

Figure 2. ORTEP drawing of $[(C_8H_{12})Rh]_2WS_4$ (**5**). Thermal ellipsoids are drawn with 50% probability boundaries.

Table I. Summary of Crystal Data and X-ray Data Collection and Reduction for $[(C_8H_{12})Rh]_2WS_4{\cdot}C_7H_8$

Crystal Parameters	
crystal system	monoclinic
space group	$P2/c$ (13)
crystal dimens, mm	0.08 × 0.24 × 0.36
a, Å	8.174 (2)
b, Å	10.261 (1)
c, Å	15.715 (2)
β, deg	98.19 (2)
V, Å^3	1304.6
Z	2
d(calcd), g cm^{-3}	2.10
abs coeff, cm^{-1}	60.4
formula	$C_{23}H_{32}Rh_2S_4W$
fw	826.43
Data Collection and Reduction	
diffractometer	Enraf-Nonius CAD4
radiation	Mo Kα (λ = 0.71073 Å), graphite-monochromated
temp, °C	23
scan method	ω–2θ
scan rate, deg/min	1–10 (variable)
maximum 2θ	50.0
index ranges	$\pm h,+k,+l$
transmission factor	0.587–0.997
no. of total reflecns	2534
no. of unique data with $I > 3.0\sigma(I)$	1756

Table II. Bond Distances (Å)[a]

atom 1	atom 2	dist	atom 1	atom 2	dist
W	S1	2.198 (1)	C1	C8	1.532 (9)
W	S2	2.203 (1)	C2	C3	1.495 (9)
Rh1	S1	2.332 (1)	C3	C4	1.473 (11)
Rh1	S2	2.321 (1)	C4	C5	1.457 (9)
Rh1	C1	2.173 (5)	C5	C6	1.403 (8)
Rh1	C2	2.168 (5)	C6	C7	1.503 (8)
Rh1	C5	2.174 (5)	C7	C8	1.439 (10)
Rh1	C6	2.184 (5)	W	Rh1	2.854 (0)
C1	C2	1.354 (9)			

[a] Numbers in parentheses are estimated standard deviations in the least significant digits.

(5) After this work was completed, a preliminary account of Rh(I) and Ru(II) thiometalates appeared: Howard, K. E.; Rauchfuss, T. B.; Rheingold, A. L. *J. Am. Chem. Soc.* **1986**, *108*, 297.

(6) Tetrathiometalate chemistry has been reviewed: D. Coucouvanis *Acc. Chem. Res.* **1981**, *14*, 201. Muller, A.; Diemann, E.; Jostes, R.; Bogge, H. *Angew. Chem. Int. Ed. Engl.* **1981**, *20*, 934. Holm, R. H. *Chem. Soc. Rev.* **1981**, *10*, 455.

(7) Siedle, A. R.; Markell, C. G.; Lyon, P. A.; Hodgson, K. O.; Roe, L. R. *Inorg. Chem.*, in press.

(8) Siedle, A. R.; Newmark, R. A.; Pignolet, L. H.; Howells, R. D. *J. Am. Chem. Soc.* **1984**, *106*, 1510.

(9) Siedle, A. R.; Howells, R. D. U.S. Patent 4556720, 1985.

(10) Clark, R. J. H.; Dines, T. J.; Proud, G. P. *J. Chem. Soc., Dalton Trans.* **1983**, 2299.

overtone and combination bands characteristic of resonance enhanced spectra. For example, in the Raman spectrum of **7**, Figure 1, are seen peaks at 315 and 460 cm^{-1}, assigned as above, 630 [2ν(Rh–S)], 765 [ν(Rh–S) + ν(W–S)], and 920 [2ν(W–S)] cm^{-1}. The presence of the 765 cm^{-1} combination band favors the assignment of the 510 nm absorption to Rh → W charge transfer as it indicates that polarization of both the Rh–S and W–S moieties are involved in the optical transition.

Structure of $[(C_8H_{12})Rh]_2WS_4$. Recrystallization of **5** from dichloromethane–toluene affords the solvate $[(C_8H_{12})Rh]_2WS_4{\cdot}C_7H_8$ whose molecular structure and numbering scheme is shown in Figure 2. A listing of important bond distances is given in Table II. The structure comprises isolated molecules which contain a crystallographic twofold axis passing through W. The WS_4 unit is essentially tetrahedral, the S1–W–S2 angle being 105.82 (5)°; the dihedral angle between the two Rh, S1, S2, W planes is constrained to be 90°. The Rh1–S1–W and Rh–S2–W angles are 78.02 (5) and 78.18 (4)°, respectively, and the S1–Rh–S2 angle is 97.96 (5)°, indicating that, if the midpoints of the C=C bonds are taken to represent donor atoms, rhodium has a slightly distorted square-planar coordination geometry.

The W–S1 and W–S2 bond lengths are 2.198 (1) and 2.203 (1) Å, respectively, shorter than in $[(Ph_2PCH_3)_2Au]_2WS_4$, which has $d(W–S)_{av}$ = 2.22 Å and the same overall molecular architecture.[1] The Rh–S1 and Rh–S2 distances are 2.332 (1) and 2.321 (1) Å, respectively, somewhat shorter than found for tetrahedral rhodium in Rh_2S_3.[12] The Rh–W separation is 2.854 (0) Å but, because of constraints imposed by the bridging sulfide ligands, it cannot be ascertained whether this represents a chemically significant metal–metal interaction.

Experimental Section

Reactions employing the $HC(SO_2CF_3)_2^-$ salts of $(Ph_3P)_3Rh^+$ and $(Ph_3P)_3Rh(CO)_2^+$[8,9] were carried out under a nitrogen atmosphere by using deoxygenated solvents; the final products are air-stable and workup was performed in air. ^1H and ^{31}P NMR spectra were obtained on a Varian XL-200 instrument; positive chemical shifts are downfield of internal $(CH_3)_4Si$ or external 85% H_3PO_4 references. Infrared spectra were obtained on Nujol mulls on a spectrometer having grating optics; peak positions are believed to be accurate to within ±5 cm^{-1}. Raman spectra were recorded on spun samples pressed into a KBr matrix, using 514.5 nm laser excitation. Frequencies reported are accurate to within ±10 cm^{-1}. Molecular weights were determined by vapor pressure osmometry in $CHCl_3$. The $Ph_3PCH_3^+$ and Ph_4As^+ salts of the thiometalate ions WS_4^{2-}, MoS_4^{2-}, and $MoO_2S_2^{2-}$ were prepared by metathesis of their NH_4^+ salts[13] and Ph_4AsCl or Ph_3PCH_3Br in water. After filtration and vacuum-drying, these were used without further purification.

$[(Ph_3P)_2Rh]_2WS_4$ (1). A solution of 0.87 g (1 mmol) of $(Ph_3PCH_3)_2WS_4$ in 15 mL of CH_2Cl_2 was added with stirring to 1.16 g of $(Ph_3P)_3Rh^+HC(SO_2CF_3)_2^-$ in 10 mL of the same solvent. After 1.5 h, ethanol was added to the reaction mixture, which was then concentrated on a rotary evaporator to provide the crude product as a maroon powder. This was purified by flash chromatography on a 8 × 1 in. Florisil column, eluting with $CHCl_3$. Addition of ethanol to the purple eluate followed by concentration under vacuum gave 0.55 g (35%) of **1** as dark purple microcrystals. IR: ν_{WS} 457, 512 cm^{-1}. Raman: 315, 475, 630, 770, 925 cm^{-1}. Anal. Calcd (Found): C, 55.2 (54.8); H, 3.8 (3.5); P, 7.9 (7.8); Rh, 13.2 (13.2); S, 8.2 (8.2); mol wt, 1566 (1514).

$[(Ph_3P)_2Rh]_2MoS_4$ (2) was similarly obtained in 63% yield. IR: 512, 530 cm^{-1}. Raman: 310, 450 cm^{-1}. Anal. Calcd (Found) C, 58.5 (58.0); H, 4.1 (3.9); P, 8.4 (8.3); Rh, 13.9 (14.2); S, 8.7 (8.6); mol wt, 1478 (1460).

$[(Ph_3P)_2Rh]_2MoO_2S_2$ (3) was prepared in 23% yield in the same way starting from $(Ph_3PCH_3)_2MoO_2S_2$. IR: 960, 525 cm^{-1}. Raman: 420, 525 cm^{-1}. Anal. Calcd (Found): C, 59.8 (60.0); H, 4.1 (4.0); P, 8.6 (8.2); Rh, 14.3 (14.6); S, 4.4 (4.3); mol wt, 1446 (1473).

$[(Ph_3P)Rh(CO)]_2WS_4$ (4). A solution of 0.26 g (0.3 mmol) of $(Ph_3PCH_3)_2WS_4$ in 7 mL of CH_2Cl_2 was added with stirring to 0.37 g (0.6 mmol) of $(Ph_3P)_3Rh(CO)_2^+HC(SO_2CF_3)_2^-$ in 5 mL of the same solvent. After 10 min, ethanol was added and the reaction mixture concentrated to give a solid product. TLC analysis (silica gel, toluene) indicated that both **1** and **4** were present. The crude product was dissolved in toluene–ethanol and slowly evaporated under a stream of carbon monoxide to give 0.2 g (61%) of orange crystalline **4**. Anal. Calcd (Found): C, 41.5 (41.0); H, 2.7 (2.7); P, 5.6 (5.1); Rh, 18.8 (19.1); S, 11.7 (12.0); mol wt, 1098 (1115). Exchange in CH_2Cl_2 with ^{13}CO produced $[(Ph_3P)Rh(^{13}CO)]_2WS_4$ (ν_{CO} (toluene) 1957 cm^{-1}), used to obtain the ^{13}C NMR spectrum.

$[(C_8H_{12})Rh]_2WS_4$ (5). A mixture of 0.49 g (1 mmol) of $[(C_8H_{12})RhCl]_2$ and 1.09 g (1 mmol) of $(Ph_4As)_2WS_4$ in 11 mL of CH_2Cl_2 was stirred for 15 min. Then ethanol was added and the solution was concentrated on a rotary evaporator to produce a crude product. This was chromatographed on a 12 × 1 in. silica gel column, eluting with CH_2Cl_2. Addition of butanone to the orange eluate and concentrating gave 0.45 g (45%) of scarlet, crystalline **5**. IR: 464 cm^{-1}. Raman: 310, 470, 775, 860, 940 cm^{-1}. ^1H NMR (CD_2Cl_2): 5.77 (4 H), 2.53 (8 H) ppm. Anal. Calcd (Found): C, 26.2 (26.4); H, 3.3 (3.3); Rh, 28.1 (28.0); S, 17.4 (17.0).

Crystals of the 1:1 toluene solvate used for the X-ray diffraction experiment were grown by slow diffusion of toluene into a CH_2Cl_2 solution of **5**.

$[(C_8H_{12})Ir]WS_4$ (6) was similarly prepared in 39% yield starting with $[(C_8H_{12})IrCl]_2$. IR: 461 cm^{-1}. Raman: 320, 470, 630, 770, 925 cm^{-1}. ^1H NMR ($CDCl_3$): 5.77 (4 H), 2.53 (8 H) ppm. Anal. Calcd (Found): C, 21.1 (21.0); H, 2.6 (2.5); Ir, 42.1 (42.0); S, 14.0 (13.7); mol wt, 912 (898).

[(diphos)Rh]$_2WS_4$ (7). A mixture of 0.16 g of **5** and 0.2 g of diphos in 15 mL of CH_2Cl_2 was stirred for 30 min. Toluene, 6 mL, was added and the solution concentrated until solids formed. After cooling to −20 °C, the product was collected on a filter and then recrystallized again from toluene. The yield of carmine crystals was 0.22 g (94%). IR: 450 cm^{-1}. Raman: 315, 460, 630, 765, 920, 1025 cm^{-1}. Anal. Calcd (Found): C, 47.5 (48.1); H, 3.7 (3.9); P, 9.4 (9.6); Rh, 15.7 (15.4); S, 9.7 (10.1); mol wt, 1314 (1297).

Table III. Positional Parameters and Their Estimated Standard Deviations[a]

atom	x	y	z	B, Å^2
W	0.500	0.28483 (3)	0.250	3.779 (7)
Rh1	0.65934 (6)	0.28884 (5)	0.09984 (3)	3.73 (1)
S1	0.4382 (2)	0.1652 (2)	0.1338 (1)	5.05 (4)
S2	0.7134 (2)	0.4046 (2)	0.2276 (1)	4.99 (4)
C1	0.5704 (9)	0.2502 (8)	−0.0348 (4)	5.4 (2)
C2	0.6734 (9)	0.1523 (7)	−0.0041 (4)	5.6 (2)
C3	0.847 (1)	0.1400 (9)	−0.0221 (6)	9.0 (3)
C4	0.972 (1)	0.226 (1)	0.0259 (7)	8.4 (3)
C5	0.9093 (8)	0.3303 (8)	0.0754 (4)	5.3 (2)
C6	0.8065 (8)	0.4332 (7)	0.0423 (4)	5.3 (2)
C7	0.747 (1)	0.4524 (9)	−0.0518 (5)	7.7 (2)
C8	0.619 (1)	0.3644 (9)	−0.0888 (5)	7.7 (2)
C9	0.000	0.250	0.750	9.1 (4)
C10	0.000	0.976 (1)	0.250	11.7 (5)
C11	0.109 (2)	0.138 (2)	0.7673 (8)	6.3 (4)
C12	0.190 (2)	0.221 (2)	0.791 (1)	7.5 (4)
C13	0.253 (2)	0.116 (2)	0.795 (1)	8.4 (4)
C14	0.126 (2)	−0.009 (2)	0.775 (1)	11.3 (6)
H1	0.4614	0.2477	−0.0219	6*
H2	0.6310	0.0885	0.0303	6*
H3	0.8824	0.0514	−0.0098	9*
H4	0.8487	0.1546	−0.0824	9*
H5	1.0357	0.2645	−0.0155	9*
H6	1.0467	0.1732	0.0636	9*
H7	0.9401	0.3294	0.1356	6*
H8	0.7743	0.4948	0.0817	6*
H9	0.7011	0.5390	−0.0591	9*
H10	0.8358	0.4446	−0.0829	9*
H11	0.5208	0.4146	−0.1056	9*
H12	0.6541	0.3290	−0.1395	9*

[a] An asterisk denotes atoms that were not anisotropically refined. Anisotropically refined atoms are given in the form of the isotropic equivalent thermal parameter defined as $(4/3)[a^2B(1,1) + b^2B(2,2) + c^2B(3,3) + ab(\cos\gamma)B(1,2) + ac(\cos\beta)B(1,3) + bc(\cos\alpha)B(2,3)]$.

Structure Determination

Details of crystal data and X-ray data collection are gathered in Table I, and atomic positional parameters are given in Table III. The data were corrected for Lorentz, polarization, and background effects[14] as well as for absorption.[15] Because three

(11) Schmidt, K. H.; Muller, A. *Coord. Chem. Rev.* **1974**, *14*, 115.
(12) Parthe, E.; Hohnke, D.; Hulliger, F. *Acta Crystallogr.* **1967**, *23*, 832.
(13) McDonald, J. W.; Friesen, G. D.; Rosenhein, L. D.; Newton, W. E. *Inorg. Chim. Acta* **1983**, *72*, 205.

intensity standards showed a loss in intensity of 12.5%, a decay correction was applied. Systematic extinctions ($h0l$, $l \neq 2n$) were consistent with the space group $P2/c$. The structure was solved by the Patterson method. Full-matrix least-squares refinement[16] and difference Fourier calculations were used to locate all remaining non-hydrogen atoms including a solvent toluene molecule. Positions of hydrogen atoms in the cyclooctadiene ligand were calculated and included in the structure factor calculations but were not refined. The toluene molecule was disordered, and a two-site model was used to describe the disorder. All non-hydrogen atoms were refined anisotropically. Because it was not possible to unambiguously locate the toluene methyl carbon atom, neither it nor the toluene hydrogen atoms were included in the final refinement, which converged (largest shift = 0.01σ) with R = 0.026 and R_w = 0.041. The final difference Fourier showed no peaks greater than 0.7 e/Å^3 (toluene region). The values of the atomic scattering factors were taken from the usual tabulation,[17] and the effects of anomalous dispersion were included.[18]

Acknowledgment. We are grateful to the staff of the 3M Analytical and Properties Research Laboratory for the spectroscopic and analytical data and to Jim Westberg, who obtained the Raman spectra.

Registry No. 1, 99594-08-8; **2**, 103835-65-0; **3**, 103835-66-1; **4**, 99594-10-2; **5**, 99594-03-3; **5**·C_6H_6, 103835-67-2; **6**, 99594-06-6; **7**, 99594-09-9; $(Ph_3P)_3Rh^+CH(SO_2CF_3)_2^-$, 88825-75-6; $[(C_8H_{12})RhCl]_2$, 12092-47-6; $[(C_8H_{12})IrCl]_2$, 12112-67-3.

Supplementary Material Available: Tables of general temperature factor expressions, bond angles, torsional angles, disordered toluene atomic coordinates, and calculated hydrogen atomic coordinates (6 pages); a listing of structure factor amplitudes (11 pages). Ordering information is given on any current masthead page.

(14) The intensity data were processed as described in: *CAD 4 and SDP User's Manual*; Enraf-Nonius: Delft, Holland, 1978. The net intensity $I = (K/\text{NPI})(C - 2B)$, where K = 20.1166 × (attenuation factor), NPI = ratio of fastest possible scan rate to scan rate for the measurement, C = total count, and B = total background count. The standard deviation is given by $\sigma^2(I) = (K/\text{NPI})^2[C + 4B + (pI)^2]$ where p is a factor (here 0.04) used to downweight intense reflections.

(15) North, B.; North, A. C. T., Phillips, D. C.; Mathews, F. S. *Acta Crystallogr., Sect. A: Cryst. Phys., Diffr., Theor. Gen. Crystallogr.* **1968**, *A24*, 351–359.

(16) All calculations were carried out on PDP 8A and 11/34 computers using the Enraf-Nonius CAD4/SDP program. This crystallographic computing package is described by Frenz (Frenz, B. A. In *Computing in Crystallography*; Schenk, H., Olthof-Hazekamp, R., van Konigsveld, H., Bassi, G. C., Eds.; Delft University Press: Delft, Holland, 1978; pp 64–71). All least-squares refinements were based on the minimization of $\sum w(|F_o| - |F_c|)^2$ where $w = 1/\sigma^2(F_o)$. The unweighted and weighted residuals are defined as $R = (\sum||F_o| - |F_c||)/\sum|F_o|$ and $R_w = [(\sum w(|F_o| - |F_c|)^2/(\sum w|F_o|)^2]^{1/2}$.

(17) Cromer, D. T.; Waber, J. T. *International Tables for X-Ray Crystallography*; Kynoch: Birmingham, England, 1974; Vol. IV, Table 2.2A. Cromer, D. T. *Ibid.*; Table 2.3.1.

(18) Cromer, D. T.; Ibers, J. A. *International Tables for X-Ray Crstallography*; Kynoch: Birmingham, England, 1984; Vol. IV, Table 2.2C.

Contribution from the Department of Chemistry, University of California, Davis, California 95616

Crystal and Molecular Structure of Chloramine-T Trihydrate. Absence of a Sodium–Nitrogen Interaction in the Oxidant *N*-Chloro-*N*-sodiotoluene-*p*-sulfonamide

Marilyn M. Olmstead and Philip P. Power*

Received April 17, 1986

The wide variety of reactions undergone by chloramine-T (the sodium salt of *N*-chloro-4-methylbenzenesulfonamide) has attracted considerable interest. Two recent reviews,[1,2] however, have referred to the lack of structural data available for this and related compounds. The structure of chloramine-T is often represented as A or, much less commonly, B. These structures convey very

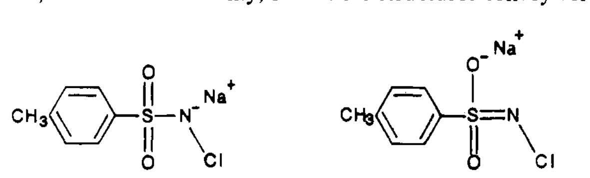

A B

different bonding descriptions. In A there is a single bond between sulfur and nitrogen and an interaction between the sodium ion and the nitrogen center. In B a sulfur–nitrogen double bond is inferred, as well as an interaction between the sodium ion and one or both oxygens. A survey of the literature does little to shed further light on a correct structural assignment. There are no X-ray structures for any $[RSO_2NCl]^-$ grouping although the structures of a number of sulfilimines $[RSO_2NR']^-$[3-5] are known. Crystal structures of nitrogen–halide-bonded compounds are also understandably rare.

In this paper we report the structure of $[Na][4\text{-}MeC_6H_4SO_2NCl]\cdot 3H_2O$, chloramine-T, and show by X-ray crystallography that there is no interaction between nitrogen and sodium. Instead the Na^+ ion interacts with one of the sulfonyl oxygens and a chlorine from a neighboring $[4\text{-}MeC_6H_4SO_2NCl]^-$ ion. The remainder of the roughly octahedral Na^+ coordination sphere involves oxygens from waters of crystallization. The structure is therefore closer to the formulation B than to its more common representation as A.

Crystal Data, X-ray Data Collection, and Solution and Refinement of Structure

The colorless crystals of chloramine-T (Aldrich) are readily obtained by slow evaporation of an aqueous or ethanolic solution of the compound. Those obtained from water grow as thin, frequently twinned plates; however, on the basis of cell dimensions, they are isomorphous with those obtained from ethanol. A parallelepiped of dimensions 0.12 × 0.32 × 0.60 mm from an ethanol recrystallization was selected for X-ray data collection. A Syntex $P2_1$ diffractometer equipped with a graphite monochromator was used. Crystal data (293 K): triclinic, a = 6.393 (1) Å, b = 7.510 (1) Å, c = 13.767 (2) Å, α = 85.33 (1)°, β = 83.92 (1)°, γ = 74.11 (1)°, V = 631.2 (2) Å^3, d_{calcd} = 1.48 g cm^{-3}, Z = 2, space group $P\bar{1}$, μ(Mo Kα) = 5.0 cm^{-1}, range of absorption correction factors 1.05–1.15. An absorption correction was applied.[6] A total of 2891 data were collected in the range of $0 < 2\theta \leq 55°$, with hkl ranges 0 to +8, −9 to +9, and −17 to +17, respectively, of which 2366 ($I > 2\theta(I)$) were used in the solution and refinement of the structure. The structure was solved by direct methods. The function minimized throughout refinement was $w(|F_o| - k|F_c|)^2$, with $w = 1/\sigma^2(F_o)$. Final refinement was carried out with anisotropic thermal parameters for all non-hydrogen atoms. The hydrogen atoms of all three H_2O molecules were allowed to refine as isotropic atoms. The phenyl ring hydrogens were refined by use of a riding model on the bonded carbon and free thermal parameters. The methyl hydrogens are subject to very large thermal motion and were included in the structure factor calculation at fixed positions obtained from a difference map and with free thermal parameters. At convergence, R = 0.039, R_w = 0.048, $w = 1/\sigma^2(F)$, and GOF = 1.04, for 176 parameters.[7] Atom coordinates, isotropic thermal parameters, bond distances, and bond angles are given in Tables I and II.

Results and Discussion

The crystal structure of chloramine-T is complex and cannot easily be described by the usual packing of molecular species. The

(1) Bremner, D. H. In *Synthetic Reagents*; Pizey, J. S., Ed.; Horwood-Wiley: New York, 1985; pp 9–59.

(2) Campbell, M. M.; Johnson, G. *Chem. Rev.* **1978**, *78*, 65–79.

(3) Cameron, A. F.; Hair, N. J.; Morris, D. G. *J. Chem. Soc., Perkin Trans. 2* **1973**, 1951–1954.

(4) Kálmán, A.; Sasvari, K. *Cryst. Struct. Commun.* **1972**, *1*, 243–246.

(5) Kálmán, A. *Acta Crystallogr.* **1967**, *22*, 501–507.

(6) Program XABS by H. Hope and B. Moezzi. The program obtains an absorption tensor from $F_o - F_c$ differences.

(7) Scattering factors and the correction for anomalous dispersion were taken from: *International Tables for X-ray Crystallography*; Kynoch: Birmingham, England, 1974; Vol. IV. Crystallographic programs used were those of SHELXTL, version 4, installed on a Data General Eclipse computer.

0020-1669/86/1325-4057$01.50/0